Effects of cadmium, inorganic mercury and methyl-mercury on the physiology and metabolomic profiles of shoots of the macrophyte Elodea nuttallii

Claudia Cosio, D Renault

HAL Id: hal-02393954

https://univ-rennes.hal.science/hal-02393954

Submitted on 3 Feb 2020
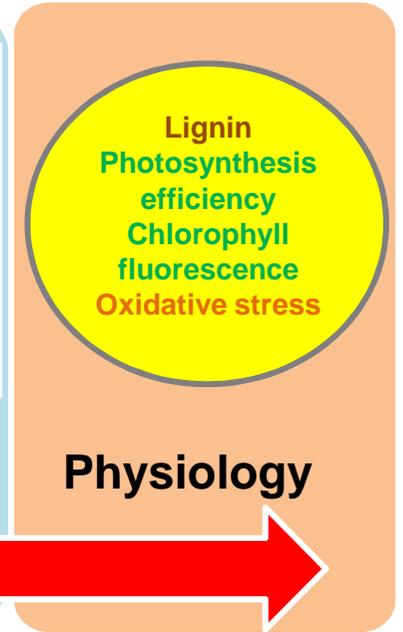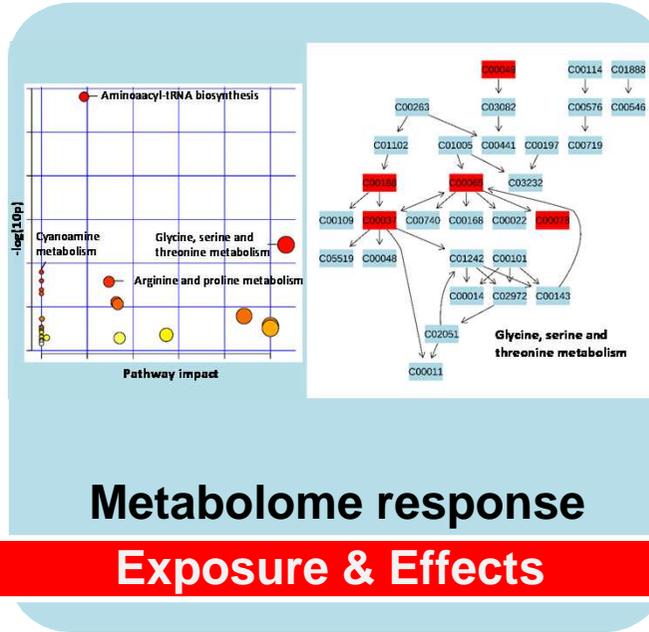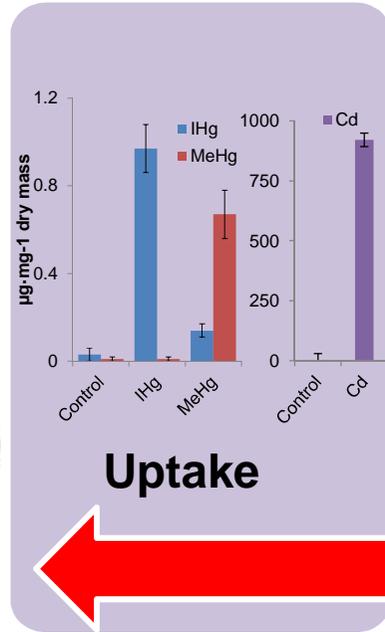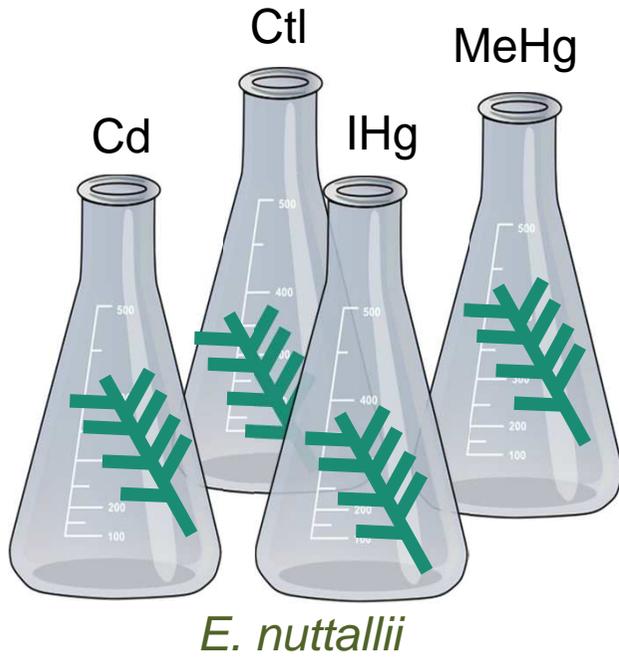
1   **Effects of cadmium, inorganic mercury and methyl-mercury on the physiology and metabolomic**

2   **profiles of shoots of the macrophyte *Elodea nuttallii***

3

4   Claudia Cosio[1,*] and David Renault[2,3]

5

6   [1] Université de Reims Champagne Ardennes, UMR-I 02 INERIS-URCA-ULH SEBIO, F-51687 Reims,

7   France

8   [2] Université de Rennes 1, UMR 6553 EcoBio CNRS, F-35042 Rennes, France

9   [3] Institut Universitaire de France, 1 rue Descartes, 75231 Paris CEDEX 05, France

10

11

12   *Corresponding author: claudia.cosio@univ-reims.fr

13 **ABSTRACT**

14 Macrophytes are known to bioaccumulate metals, but a thorough understanding of tolerance

15 strategies and molecular impact of metals in aquatic plants is still lacking. The present study aimed

16 to compare Hg and Cd effects in a representative macrophyte, *Elodea nuttallii* using physiological

17 endpoints and metabolite profiles in shoots and cytosol.

18 Exposure 24h to methyl-Hg (23 ng·L^{-1}), inorganic Hg (70 ng·L^{-1}) and Cd (281 µg·L^{-1}) did not affect

19 photosynthesis, or antioxidant enzymes despite the significant accumulation of metals, confirming a

20 sublethal stress level. In shoots, Cd resulted in a higher level of regulation of metabolites than MeHg,

21 while MeHg resulted in the largest number of regulated metabolites and IHg treatment regulated no

22 metabolites significantly. In cytosol, Cd regulated more metabolites than IHg and only arginine,

23 histidine and mannose were reduced by MeHg exposure. Kyoto Encyclopedia of Genes and Genomes

24 (KEGG) pathway analysis of data suggested that exposure to MeHg resulted in biochemical changes

25 including aminoacyl-tRNA biosynthesis, glycine, serine and threonine metabolism, nitrogen

26 metabolism, arginine and proline metabolism, cyanoamino acid metabolism, while the treatment of

27 Cd stress caused significant variations in aminoacyl-tRNA biosynthesis and branched-chain amino

28 acids pathways. Data supports an impact of MeHg on N homeostasis, while Cd resulted in an osmotic

29 stress-like pattern and IHg had a low impact. Marked differences in the responses to MeHg and IHg

30 exposure were evidenced, supporting different molecular toxicity pathways and main impact of

31 MeHg on non-soluble compartment, while main impact of IHg was on soluble compartment.

32 Metabolomics was used for the first time in this species and proved to be very useful to confirm and

33 complement recent knowledge gained by transcriptomics and proteomics, highlighting the high

34 interest of multi-omics approaches to identify early impact of environmental pollution.

35

37

38 **Capsule:** Metabolomics reveal different cellular toxicity responses to sublethal Cd, MeHg and IHg

39 treatment in *Elodea nuttallii*

40

41   **1. INTRODUCTION**

42   Anthropogenic activities result in environmental contamination by mercury (Hg) and cadmium (Cd)

43   (Loizeau et al., 2013; Azimi and Rocher, 2016)*.* As a result, biota is affected by the toxicity of these

44   toxic metals, which can also affect human populations *via* contaminated food (Croteau et al., 2005;

45   Bravo et al., 2010; Niane et al., 2014). Metals can enter the food chain through primary producers,

46   including macrophytes, which represent a key group within communities of shallow water, in terms

47   of biomass, primary production, food source and shelter for fauna. Importantly, macrophytes are

48   also central to oxygen, pollutants and nutriments biogeochemical cycles (Wetzel, 2001; Chambers et

49   al., 2008; Bonanno and Lo Giudice, 2010; Noges et al., 2010). High levels of Cd, inorganic Hg (IHg)

50   and methyl-Hg (MeHg) can be observed in aquatic ecosystems colonized by plants (Samecka-

51   Cymerman and Kempers, 2003; Castro et al., 2009; Regier et al., 2013b). Therefore, bioaccumulation

52   of metals in macrophytes represents a significant and current environmental concern (Beauvais-

53   Fluck et al., 2016; Beauvais-Fluck et al., 2017).

54   Due to their ability to accumulate and tolerate high concentrations of metals (Regier et al., 2013b;

55   Cosio et al., 2014), aquatic plants are often seen as good candidates for phytoremediation,

56   biomonitoring and ecotoxicology investigations (Valega et al., 2009; Bonanno and Lo Giudice, 2010;

57   Cosio et al., 2014). However, physiological mechanisms associated with metal accumulation and

58   prevention of their toxicity are still poorly understood in those plants, preventing the full

59   optimization of their use for environmental applications. Increasing the knowledge on the biology

60   and physiology of these plants, and more particularly the impact of metal accumulation on their

61   metabolism is therefore a research priority (Cosio et al., 2014).

62   *Elodea nuttallii* is a macrophyte widely distributed in temperate regions, and it is well-known for its

63   accumulative capacity of metals (Larras et al., 2013; Regier et al., 2013b). Several recent studies used

64   transcriptomics and proteomics approaches to describe cellular toxicity of Cd and Hg in *E. nuttallii*,

65   with the aim of using this plant for active biomonitoring. Data revealed rapid molecular changes in

66   metal-exposed plants (Larras et al., 2013; Regier et al., 2013a; Regier et al., 2013b; Regier et al.,

67   2016; Beauvais-Fluck et al., 2018a; Beauvais-Fluck et al., 2018b). These studies, spanning a wide

68   range of concentrations, globally suggest toxic metals to impact genes and proteins involved in cell

69   structure (lignin content), energy metabolism (sugar and photosynthesis), amino acid metabolism,

70   and to trigger anti-oxidative stress responses (Larras et al., 2013; Regier et al., 2013a; Regier et al.,

71   2013b; Regier et al., 2016; Beauvais-Fluck et al., 2018b). Besides, several differences were observed

72   between IHg and MeHg responses. At the transcriptome level, MeHg deregulated more genes than

73   IHg at similar intracellular concentrations (Beauvais-Fluck et al., 2018b). At the proteome level, 200

74   ng·L^{-1} IHg had a significant and similar effect than 500 µg·L^{-1} Cd exposure, while 30 ng·L^{-1} MeHg was

75   similar to controls, showing non-significant changes in proteome (Larras et al., 2013). Data thus

76   suggest different cellular toxicity pathways for IHg and MeHg. However, for both transcriptomic and

77   proteomic, many regulated contigs or peptides had an unknown function indicating considerable

78   potential for new discoveries in the biology of toxic metals.

79   Views obtained from transcriptomics, proteomics and physiological studies depict distinct levels of

80   regulation that exist in the organism. Transcriptomic informs on the level of expression of genes, but

81   cellular functions of a particular gene are carried out by its protein. Regulation of proteins in turn

82   results in alterations in levels of small metabolites involved in biochemical reactions in the functional

83   organism. Gene regulation might happen to maintain protein levels, whereas changes in the

84   abundance of proteins can be related to posttranslational modifications of proteins. Eventually,

85   proteins carry out a myriad of functions within the cell, including the metabolism of small molecules

86   such as amino acids and sugars, known to have functional roles in plant abiotic stress tolerance and

87   signaling (Yancey, 2005). Physiological adjustments and degradation of pollutants is thus ultimately

88   sustained by the metabolic network, whose production of energy, and primary and secondary

89   metabolites, are central for physiological repair and remodeling of cells. In this context,

90   metabolomic enables a large physiological representation of the effect of pollutants by incorporating

91   metabolic fluxes, enzymatic kinetics, and the resulting action of the stressors at organismal level.

92   Metabolic reconfigurations in plants exposed to pollutants, and more generally to a range of abiotic

93   stressors, result in the up-regulation and down-regulation of specific metabolic functions to sustain

94   biological functions (sustainers) and control/modulate metabolite fluxes (modulators) (Topfer et al.,

95   2014; Tohge et al., 2015).

96   In this context, metabolomics give the opportunity to confirm or reveal effects of toxicants in a way

97   that cannot be fully exploited by other molecular approaches (*e.g.* proteomics and transcriptomics).

98   In the present study, we analyzed the metabolic profiles of cytosol and shoots in *E. nuttallii* exposed

99   to Cd, IHg or MeHg, and their control counterparts, to obtain a comprehensive phenotyping of the

100   effects of sublethal concentrations of these toxicants. Metal uptake and physiological endpoints

101   were also measured. We hypothesized that amino acids and sugars should be associated with the

102   high tolerance of *E. nuttallii* to toxic metals, and thus, should be measured in higher amounts in

103   metal-exposed plants.

104

105   **2. EXPERIMENTAL SECTION**

106   **2.1. Lab-ware and reagents**

107   All laboratory material was soaked in 10% v/v HNO$_3$ (*pro analysis*, Merck, Nyon, Switzerland)

108   followed by two 10% v/v HCl (*pro analysis*, Merck, Nyon, Switzerland) acid baths for ≥ 1 week,

109 thoroughly rinsed with ultrapure water (<18.2 MΩ, MilliQ Direct system, Merck Millipore,

110 Darmstadt, Germany) and dried under a laminar flow hood. MeHg (CH₃HgCl) standard solution (1 g·L⁻

111 ¹) was obtained from Alfa Aesar (Ward Hill, MA, USA), while IHg (Hg(NO₃)₂) and Cd (Cd(NO₃)₂)

112 standard solutions (1 g·L⁻¹) were obtained from Sigma-Aldrich (Buchs, Switzerland).

113

114 **2.2. Plant culture and exposure to toxic metals**

115 Shoots of *Elodea nuttallii* (Planch.) St. John were collected in Lake Geneva (Switzerland, N46° 16'

116 28.7" E6° 10' 15.7"), and a culture was established and maintained in microcosms as previously

117 described (Regier et al., 2013b). Cultures and experiments were conducted in the laboratory under

118 controlled conditions (20 °C, 16/8 h with 5.84 W m⁻² photosynthetically active radiation [PAR], 1000

119 lux, 20 ± 1 °C). We exposed (or not: control) for 24h in triplicate three 10 cm-long shoots without

120 roots in 1L bechers filled with 1.2 µm filtered Lake Geneva water spiked with 30 ng·L⁻¹ MeHg

121 (nominal concentration 30 ng·L⁻¹, effective concentration 23 ± 7 ng·L⁻¹ MeHg), 70 ng·L⁻¹ IHg (nominal

122 concentration 200 ng·L⁻¹, effective concentration 70 ± 14 ng·L⁻¹ IHg) or 280 µg·L⁻¹ Cd (nominal

123 concentration 500 µg·L⁻¹, effective concentration 281 ± 24 µg·L⁻¹ Cd).

124

125 **2.3. Hg and Cd uptake**

126 After the 24h-long exposure to toxic metals, shoots were rinsed with 1 mM EDTA for IHg or Cd

127 treatments, and with 1 mM EDTA + 1 mM cysteine for MeHg treatments, to assess intracellular

128 metal concentrations (*i.e.* not extractable portion) (Larras et al., 2013).

129 For total Hg (THg = IHg + MeHg), lyophilized shoots of *E nuttallii* were analyzed by AMA-254. For

130 MeHg, shoots were ground, freeze-dried, and extracted by HNO₃ leaching/CH₂Cl₂ extraction. Then,

131 they were analyzed by ethylation onto Tenax traps, followed by GC separation and cold vapor atomic

132 fluorescence spectrometry (GC-CV-AFS), as described in Liu et al. (2012). For Cd, shoots were

133 ground, freeze-dried and analyzed by ICP-MS (HP 4500, Agilent) after mineralization into 4 mL HNO₃

134 *s.p.* and 1 mL H₂O₂ *s.p*.

135 THg and Cd in cytosol (see cytosol extraction protocol below) were measured by cold vapor atomic

136 fluorescence spectroscopy (CV-AFS, 2500 Tekran) and ICP-MS, respectively. MeHg in cytosol was

137 measured by the hydride generation method with cryogenic trapping, gas chromatography and

138 atomic fluorescence spectrometry (CT-GC-AFS) (Stoichev et al., 2004).

139 For all metal analysis methods, the analytical quality was assured by analyzing certified reference

140 material, blanks and several samples twice.

141

142 **2.4. Physiological endpoints**

143 Chlorophyll content was measured by spectrophotometry (Cosio and Dunand, 2010). Chlorophyll

144 fluorescence allows determining PSII efficiency, and was measured using a Handy PEA fluorimeter

145 (Hansatech Instruments Ltd, Norfolk, UK). Plants were dark adapted for 15 min before illuminating

146 them for 1 sec while recording increase in fluorescence. The performance index PI(abs) was

147 calculated from measured fluorescence. The activities of class III peroxidases (POD) and superoxide

148 dismutases (SOD) were assessed by spectrophotometry (Cosio and Dunand, 2010; Regier et al.,

149 2016). Lignin content was measured by thyoglycolic attack (Cosio and Dunand, 2010).

150

151   **2.5. Cytosol extraction**

152 Fresh plants were prepared as described in Regier et al. (2013b). Briefly, fresh plants were all

153 collected at the same time, and weighed before being ground into 10 mL buffer (0.25M sucrose, 1

154 mM DTT, 50 mM Tris HCl pH 7.5). The resulting mixture was centrifuged at 500 g for 5 min at 4 °C.

155 Supernatant, which contained cytosol, was collected and frozen until further used for analysis of

156 metabolite concentrations. The dry mass of the whole shoots was calculated from the fresh biomass

157 of each shoot weighed before the sap extraction based on previous observations that dry mass

158 represents in average 18.3% of fresh mass for shoots.

159

160   **2.6. Analysis of metabolites**

161 For metabolomics, shoots of the plants exposed to the different experimental conditions for 24h

162 were all collected at the same time, and immediately frozen in liquid nitrogen. Shoot were kept

163 frozen at -30 °C until analysis. Three independent replicates, consisting of a pool of three shoots, or

164 corresponding to the pooled cytosols of three plants (see section 2.5 for the method used for cytosol

165 extraction), were run for each experimental condition. The plant samples were homogenized into

166 600 µL of ice-cold (-20 °C) methanol-chloroform solution (2:1, v:v) using a tungsten-bead beating

167 apparatus (RetschTM MM301, Retsch GmbH, Haan, Germany) at 25 agitations per second for 1.5

168 min. Then, a volume of 400 µl of ice-cold ultra-pure water was added to each sample, and samples

169 were subsequently vortexed and centrifuged at 4000 g for 10 min at 4 °C. A volume of 600 µL of the

170 upper aqueous phase (which contained polar metabolites) was transferred to new microtubes, and

171 further used for GC-MS and LC assays.

172

173 *GC-MS Analyzes*

174 Sixty (cytosol) or 120 (shoots) µL of the upper aqueous phase were transferred to new glass vials,

175 and these aliquots were vacuum-dried (MiVac, Genevac Ltd., Ipswitch, England) at 32 °C for 45 min.

176 Then, we used the derivatization process and GC-MS settings described in Khodayari et al., (2013).

177 Briefly, the dried aliquots were resuspended in 30 µl of 20 mg·L^{-1} methoxyamine hydrochloride

178 (Sigma-Aldrich, St. Louis, MO, USA) in pyridine, incubated under automatic orbital shaking at 40 °C

179 for 90 min. Subsequently, 30 µl of N-methyl-N-(trimethylsilyl) trifluoroacetamide (MSTFA; Sigma)

180 was added and the derivatization was conducted at 40 °C for 45 min under agitation. Our GC-MS

181 system consisted of a Trace GC Ultra chromatograph and a Trace DSQII quadrupole mass

182 spectrometer (Thermo Fischer Scientific, see Khodayari et al., (2013) for more details). Randomized

183 sample sequences were established for sample injection, chromatograms were deconvoluted using

184 *XCalibur* v2.0.7. Standard samples, consisting of 62 pure reference compounds at 1, 2, 5, 10, 20, 50,

185 100, 200, 500, 750, 1000, and 1500 µM were run, and metabolite levels were quantified using the

186 quadratic calibration curves for each reference compound.

187

188 *LC analyzes*

189 Amino acid analysis was adapted from Renault et al. (2010) and (2016). Briefly, 100 µL of the

190 metabolites in solution in the methanol-ultra-pure water extract was vacuum-dried (MiVac, Genevac

191 Ltd., Ipswitch, England) at 32 °C for 30 min, and the pellet was re-suspended into 100 µL of ultra-

192 pure water. Then, aliquots (10 µL) of the aqueous extracts were used for amino acids derivatization

193 according to the AccQ•Tag ultra derivatization kit protocol (Waters Corporation, Milford, MA).

194 Amino acids were analyzed using an Acquity UPLC®533 system (Waters Corporation, Milford, MA) by

195 injecting 1 µL of the derivatization mix onto an Acquity UPLC®534 BEH C18 1.7 µm 2.1 x 100 mm

196 column heated at 55 °C. External standards were run and used for the drawing of calibration curves,

197 further allowing the quantification of the metabolites from the samples.

198

199 **2.7. Data Analysis**

200 Principal component analysis (PCA) was performed to identify patterns in response of variables and

201 individuals, and compare the responses of the plants exposed to the three metal treatments, and

202 the control. PCA were conducted with the packages FactoMineR (http://factominer.free.fr/) and

203 ade4 (http://pbil.univ-lyon1.fr/ade4) in the R software (http://www.r-project.org). Normality and

204 homoscedasticity were tested, and a student's t-test was used in Excel (Microsoft, Redmond, WA,

205 USA) to determine if two sets of data were significantly different. For the metabolic pathway

206 analysis, the name of compounds that exhibited significant variations were analyzed in

207 MetaboAnalyst (http://www.metaboanalyst.ca). The library of metabolic pathways was assembled

208 from the KEGG database, and the significance of the pathway name was assessed with the Holm-

209 Bonferroni method.

210

211 **3. RESULTS**

212 **3.1. Bioaccumulation of metals in the plants and effects on physiological endpoints**

213 The 24h-exposure of *E. nuttallii* to Cd, IHg and MeHg resulted in a significant bioaccumulation of

214 metals in shoots (Table 1). Yet, this accumulation had no significant impact on measured

215 physiological endpoints: lignin and chlorophyll contents, photosynthesis, POD and SOD activities,

216 whose values were non-significantly different from control plants (Table 1).

217

218 **3.2. Metabolites in shoots**

219 We investigated the impact of short sublethal exposures to Cd, IHg and MeHg on the metabolic

220 phenotypes of shoots of *E. nuttallii* (Table S1). In whole shoots, Cd treatment increased the

221 concentrations of 11 amino acids, two sugars, one polyol (adonitol) and one organic acid (pipecolic

222 acid), and reduced the amounts of two amino acids (aspartic acid, methylcysteine), relative to

223 control plants. Most strongly up-regulated amino acids by Cd included leucine, isoleucine and

224 tryptophan showing a 16× increase, and tyrosine as well as valine showing 11× and 10× increase,

225 respectively, after 24h of exposure to metals. Aspartic acid and methylcysteine were reduced

226 0.05× and 0.3×, respectively by the 24h exposure to Cd. Similarly, MeHg exposure increased the

227 amounts of ammonium and of 13 amino acids, and reduced the concentration of one polyol (arabitol

228 0.5×) (Table 2). Most strongly up-regulated amino acids included BABA (4×), tryptophan and

229 methionine (2×). Exposure to IHg had no significant impact on concentrations of the measured

230 metabolites in shoots, as compared with control plants.

231 Principal component analysis (PCA) was performed to compare metabolic profiles among

232 treatments: 52% of the total variance was explained on axes 1 and 2 (Figure 1A and S1). In this PCA,

233 Cd-exposed shoots showed the most distinct pattern, while centroids of IHg and MeHg-treated

234 shoots were relatively similar to controls. Axis 1 was mainly constructed by the variations of

235 adonitol, maltose, isoleucine, valine, tryptophan, tyrosine and leucine. Axis 2 was mainly supported

236 by the variations of galactonolactone, glycerol, phosphoric acid, galactose, asparagine, glucose-6-

237 phosphate and glyceric acid. In shoots, the metabolic pathway analysis performed thanks to KEGG

238 databases revealed two biological metabolic pathways regulated by Cd: aminoacyl-tRNA

239 biosynthesis, and valine, leucine and isoleucine biosynthesis. IHg had no significant impact at the

240 level of pathways, while MeHg significantly impacted five metabolic pathways: aminoacyl-tRNA

241 biosynthesis, glycine, serine and threonine metabolism, nitrogen metabolism, arginine and proline

242 metabolism, cyanoamino acid metabolism.

243

244 **3.3. Metabolites in the cytosol**

8

245 Because amino acid and sugars transfer happens at the cellular level, we also investigated the

246 impact of short sublethal exposures to Cd, IHg and MeHg on the metabolic phenotypes in the cytosol

247 of *E. nuttallii*. Many amino acids are synthesized in the chloroplast and transported into the cytosol

248 for protein and secondary metabolite synthesis, or transported and stored in the vacuole. Similarly,

249 the transport of sugars and distribution of metabolites between compartments is coordinated in

250 plants to drive growth and development. In the cytosol of plants, treatments significantly modified

251 the concentration of several metabolites (Table 3): amounts of ammonium (1.7×), glycine (2.2×),

252 hydroxyproline (1.6×) and phosphoric acid (2.2×) were increased by exposure to Cd. Concentrations

253 of alpha-alanine (0.6×), aspartic acid (0.5×), galactose (0.4×), and mannose (0.3×) were reduced in

254 Cd-exposed plants. Ammonium concentration rose by 1.6× in plants exposed to IHg, while this

255 exposure reduced the amount of arginine (0.2×). In MeHg-exposed plants, changes of the

256 concentration of individual amino acids, relative to controls, were significantly reduced for histidine

257 (completely depleted) and arginine (0.2×). Regarding sugars, mannose was also reduced by IHg

258 (0.6×) and MeHg (0.3×), and galactose by MeHg (0.3×). No significant variation was reported at the

259 level of the metabolic pathways in the cytosol of the treated plants, as compared with control

260 plants.

261 Principal component analysis of metabolites in cytosol explained 60% of the variance of samples on

262 the first and second axes (Figure 1B and S2). Plants exposed to Cd showed the most distinct

263 metabolic phenotypes relative to control plants on both axes 1 and 2. While MeHg-treated plants

264 were separated from controls on axis 2, the centroid of IHg-treated plants was close to the one of

265 their control counterparts. The first axis of the PCA was mainly supported by the variations of

266 tryptophan, valine, proline, glutamic acid, phenylalanine, GABA and threonine. The second axis was

267 constructed by the variations of glucose, galactose, mannose, alpha-alanine, inositol, aspartic acid

268 and fructose.

269

270 **4. DISCUSSION**

271 **4.1. Bioaccumulation and physiological endpoints**

272 Both bioaccumulation and physiological endpoint analyses confirmed that metal concentrations

273 used here resulted in their significant bioaccumulation, with sublethal effects for *E. nuttallii*, as

274 earlier reported in other studies (Larras et al., 2013; Regier et al., 2013b; Beauvais-Fluck et al.,

275 2018b). Chosen concentrations of metal in our work are representing a compromise between high

276 concentrations resulting in unambiguous metal accumulation pattern in macrophytes, and

277 concentrations with environmental relevance. Earlier investigations using the same concentrations

278 of Cd (281 µg·L^{-1}) and IHg (70 ng·L^{-1}) for 7d revealed that root growth was reduced, while lignification

279 of stems was increased in *E. nuttallii* (Larras et al., 2013). Nevertheless, these treatments had no

280 effects on chlorophyll content and shoot growth (Larras et al., 2013; Regier et al., 2013b).

281 Conversely, exposure to MeHg (23 ng·L^{-1}) for 7d increased root growth, suggesting a hormesis effect

282 that is seen as an overcompensation of a moderate stress (Larras et al., 2013). Similarly in another

283 study, exposure for 2h to 10 ng·L^{-1} or 10 µg·L^{-1} MeHg had no significant effect on chlorophyll content,

284 POD and SOD activities in *E. nuttallii* (Beauvais-Fluck et al., 2018b). In sum, consistent with the

285 literature and based on the absence of effects of the physiological endpoints, our experimental

286 conditions did not induce an acute stress in *E. nuttallii* shoots. Eventually, these data confirmed that

287 *E. nuttallii* is highly tolerant to metals.

288

289 **4.2. Effects of metals on the metabolic phenotypes of macrophytes**

290 We were interested in obtaining a general picture of effects of toxic metals on the physiology of the

291 plants by comparing their metabolic signatures. Our metabolic profiling revealed that all treatments

292 impacted metabolite amounts in shoots, cytosol or both, as compared with control plants. The Cd-

293 treated plants were characterized by the most distinct metabolic phenotypes according to PCA, in

294 both shoots and cytosol. This finding highlights a higher impact of this metal on the amount of each

295 metabolite, as also evidenced by a higher level of regulation (up to 16×) than the one measured in

296 IHg and MeHg treatments. Even if this distinction may partially result from the higher Cd

297 concentration used as compared with IHg and MeHg, we must re-emphasize that we did not find

298 differences among the three treatments and the control for the other physiological endpoints.

299 Moreover, metabolic pathway analysis suggested that MeHg impacted more metabolic pathways in

300 shoots than did Cd in our experimental conditions. A previous proteomic study with identical

301 experimental conditions suggested similar responses, and stress-induced level of IHg and Cd in *E.*

302 *nuttallii*, and an absence of response for MeHg (Larras et al., 2013). Conversely, transcriptomic

303 analyses suggested similar stress levels for Cd and IHg and a higher molecular impact of MeHg

304 (Regier et al., 2013a; Beauvais-Fluck et al., 2018b). When examining responses of the two considered

305 compartments (shoots and cytosol), we observed that Cd and MeHg both significantly impacted

306 several pathways in shoots, while IHg had no significant impact on metabolites pathways. For

307 cytosol, Cd had a higher impact than IHg, while MeHg had lower impact than IHg. Both cytosolic

308 compartment analysis and proteomics target soluble molecules, suggesting that IHg might impact

309 mainly soluble compartments, while MeHg impacts mainly the non-soluble compartments. However,

310 these differences reflect different molecular toxicity pathways of the three metals, and highlight the

311 interest of coupling analysis at different levels of organization. Indeed, the present study brings a

312 different pattern as compared with those previously observed by transcriptomics. For instance,

313   MeHg was earlier reported as a stronger dysregulator than IHg, by affecting a much higher number

314   of genes in *E. nuttalli* (Beauvais-Fluck et al., 2018b). In our study, metabolomics confirmed that

315   MeHg has a stronger molecular effect than IHg in shoots, but not in cytosol. In addition, Cd, IHg, and

316   MeHg regulated genes involved in biosynthesis of sulfur-containing amino acids such as methionine

317   and cysteine (Regier et al., 2013a; Beauvais-Fluck et al., 2018a; Beauvais-Fluck et al., 2018b).

318   Methionine was increased 2× by MeHg in shoots supporting its role in MeHg response, while

319   cysteine was not altered after metal exposure in shoots or cytosol, suggesting that regulation at the

320   gene and protein level was mostly happening to maintain the level of this metabolite.

321

322   **4.3 Early signs of stress responses in *Elodea nuttalli* treated with Cd**

323   Exposure of *E. nuttalli* resulted in a significant re-patterning of the metabolic phenotype, with for

324   instance a significant effect on the concentrations of metabolites involved in aminoacyl-tRNA

325   biosynthesis, and on the branched-chain amino acids. Aminoacyl-tRNA biosynthesis is involved in the

326   synthesis of proteins in organisms, and are particularly central to growth (Banerjee et al., 2011;

327   Raina and Ibba, 2014). Most often, the activity of this pathway declines when plants are exposed to

328   stressful or restrictive conditions, as requirements for protein synthesis is reduced to favor the

329   activation of stress-response genes (Holcik and Sonenberg, 2005). In parallel, we also found that Cd

330   treatment impacted the concentration of branched-chain amino acids (*i.e.* leucine, isoleucine and

331   valine) in shoots of *E. nutalli*. Branched-chain amino acids share four enzymes for their biosynthesis,

332   which are coordinately regulated. Plants that accumulate and tolerate high Cd amounts, such as

333   *Solanum nigrum*, have been demonstrated to accumulate isoleucine and valine in roots (Xu et al.,

334   2012). Branched amino acids derive from the shikimate pathway, and are required for protein

335   synthesis and production of aromatic secondary metabolites, *e.g.* flavonoids, lignin cell wall

336   components, and anthocyanins, which are important for cell wall extensibility and non-enzymatic

337   anti-oxidative response both involved in metal tolerance in plants (Tzin and Galili, 2010; Zemanova

338   et al., 2017). Branched-chain amino acids also serve as precursors for the production of secondary

339   metabolites (*e.g.* alkaloids, glycosides) involved in responses to biotic and abiotic stress (Rizhsky et

340   al., 2004). These secondary metabolites notably play a role during osmotic stress (Zemanova et al.,

341   2017). Our metabolite profiling thus suggests that Cd exposure results in an osmotic stress to *E.

342   nuttallii*, as depicted by the 10× to 16× increase of leucine, isoleucine and valine that typically

343   accumulate in osmotically challenged plants. This hypothesis is further supported by the significant

344   accumulation of proline, a well-known biomarker of water stress in plants. Indeed, proline can act as

345   an osmolyte, a metal chelator, an antioxidative defense molecule and a signaling molecule (Hayat et

346   al., 2012).

347   The probable osmotic stress induced by Cd-exposure likely increased the amount of oxidative stress

348   experienced by the plants. Oxidative stress has been shown to alter the activity of the Krebs cycle

349   (Obata and Fernie, 2012), with potential side effects on the pathway connected to the TCA, and thus

350   on the levels of TCA-cycle-derived compounds. This includes aspartic acid, whose levels decreased in

351   shoots (and to a lesser extent in the cytosol) of Cd-treated plants. Besides, we also measured

352   decreased amounts of mannose and galactose in shoots of *E. nuttalli*. These two sugars are involved

353   in the Smirnoff-Wheeler pathway, and their reduction suggests that they were used for the

354   biosynthesis of ascorbic acid. Ascorbic acid is widely recognized as an important ROS scavenger in

355   plants, and earlier studies reported that accumulation or enhanced production of ascorbic acid

356   boosted the ability of plants to cope with salt or drought stress, by limiting the peroxidation of

357   membrane lipids and reducing losses of the chlorophyll content (Venkatesh and Park, 2014).

358   Increased ROS production in Cd-treated plant is very likely, as this is a reported toxic effect of metal

359   exposure at higher concentrations (Kieffer et al., 2009; Xu et al., 2012; Larras et al., 2013).

360   Finally, the accumulation of leucine, isoleucine and valine may serve to promote stress-induced

361   protein synthesis, and may act as signaling molecules to regulate gene expression (Joshi et al., 2010).

362   The breakdown products of these three amino acids, *e.g.* acetyl-CoA, propionyl-CoA, and

363   acetoacetate, are potential energy sources for plants (Joshi et al., 2010). The global increase of

364   numerous amino acids likely depicts increased degradation and synthesis of proteins (Vital et al.,

365   2017). Similar observation was reported in crop cultivars, and shown to be linked to impact of

366   osmotic stress on the proteasome (Vital et al., 2017).

367

368   **4.4. MeHg affects the nitrogen metabolism and triggers chemical defenses against abiotic**

369   **stress**

370   In macrophytes exposed 24h to MeHg, the amount of several amino acids, including aspartic acid,

371   glutamine, glycine, phenylalanine, proline, threonine and tryptophan were altered in shoots. This

372   finding is congruent with previous transcriptomic studies conducted on *E. nuttallii* exposed to MeHg,

373   which showed that genes involved in synthesis of proteins represented a high proportion of

374   regulated genes (Beauvais-Fluck et al., 2018a). Altogether, data suggest a rapid adjustment of the

375   plants to MeHg exposure. Several of these amino acids are expected to have a role in chemical

376   defenses against abiotic stresses, notably glycine, threonine and proline (as discussed above).

377   Our metabolomic data, and more particularly the significant rise of glutamine and ammonium

378   amounts, further support that MeHg affects nitrogen (N) metabolism and homeostasis in the plant.

379   The increase of the amount of aspartatic acid and glutamine in MeHg-treated plants, and the

380   concomitant reduction of ammonium amount in cytosol, suggest that N transport is altered. In

381   plants, the main pathway of ammonia assimilation is the GS/GOGAT cycle, where glutamine

382   synthetase / glutamate synthase cooperate (Masclaux-Daubresse et al., 2006). Plants may also

383   utilize the reaction catalyzed by glutamate dehydrogenase for ammonia assimilation, especially

384   under environmental stress conditions (Masclaux-Daubresse et al., 2006). Consequently, in plants,

385   aspartic acid, asparagine, glutamic acid and glutamine are the main amino acids transporter of N

386   (Miesak and Coruzzi, 2002). Here, the increase in ammonia and glutamine (high N/C ratio) suggest

387   that nitrate assimilation is affected, and both ammonia and amino acids are released by protein

388   degradation and hydrolysis. Similarly, previous transcriptomic study in *E. nuttallii* exposed to IHg,

389   MeHg or Cd highlighted a down-regulation of genes coding for nitrate and ammonium transport (e.g.

390   high affinity nitrate transporters) suggesting a global impact of tested metals on nutrition (Regier et

391   al., 2013a; Beauvais-Fluck et al., 2018a).

392   Phenylalanine, threonine, and tryptophan are aromatic amino acids coupled with the

393   phenylpropanoid and the shikimate pathways. Phenylpropanoids are a diverse group of compounds

394   derived from the carbon skeleton of phenylalanine. These compounds are involved in plant defense

395   and generate cell wall components (*e.g.* lignin) and antioxidant metabolites (*e.g.* anthocyanin)

396   (Fraser and Chapple, 2011). In previous study, a significant increase of anthocyanin, acting as non-

397   enzymatic antioxidants (Beauvais-Fluck et al., 2018a; Beauvais-Fluck et al., 2018b), was measured in

398   *E. nuttallii* exposed 2h to 10 ng·L^{-1} MeHg and higher concentrations, but not after IHg treatments

399   (Beauvais-Fluck et al., 2018b). The increase amount of phenylalanine, threonine, and tryptophan

400   suggests enhanced antioxidant activity in MeHg-treated plants.

401

402   **4.5. Toxic metals had little effects on the concentration of sugars**

403   A previous study hypothesized that the accumulation of fructose, galactose, sucrose and glucose in

404   poplar (*Populus tremula* L.) exposed to Cd might act as osmoprotectants playing critical roles in

405   osmotic adjustments, and protection of cell membranes against toxic trace metals (Kieffer et al.,

406   2009). Here, exposures decreased mannose and galactose amounts in cytosol. Both sugars are

407   involved in the ascorbic acid biosynthetic pathway, a major antioxidant in higher plants, and their

408   decrease is thus in line with expected cellular toxicity of metals (Ma et al., 2014). Other studies

409   suggested cellular adjustments to control resources distribution within cells: reduced sugar

410   utilization in the presence of Cd and consequently photoassimilates partial storage as sugars (Moya

411   et al., 1995; Bailey et al., 2003). In the aquatic plant *Wolffia arrhizal*, sugar and protein contents

412   were negatively correlated with toxic metal concentrations (Piotrowska et al., 2010; Zhang et al.,

413   2017). In the same line, sugars accumulated in correlation with a decline of net photosynthetic rates

414   in rice exposed to Cd (Moya et al., 1995). Similarly, amino acid metabolism often is expected to be

415　closely related to abiotic stress tolerance (Zhang et al., 2017). However, in our study few sugars

416　varied between treated and control plants, both in cytosol and shoots. Nevertheless, we observed

417　an increase of sugars in shoots, while their content concomitantly decreased in cytosol. The

418　transport of sugars and distribution between storage, respiration and biosynthesis in sink tissues are

419　coordinated activities in plants (Rosa et al., 2009a; Lemoine et al., 2013). Stress-related increase in

420　sugar delivery to sinks is important for growth, cell turgor and water potential maintenance

421　(Lemoine et al., 2013). Besides, soluble sugars have several roles in cells, including as metabolic

422　resources, structural constituents of cells, but also in stress signaling (Rosa et al., 2009b).

423　Transporters are required for efficient movement of sugars that are polar solutes across membranes

424　(Patrick et al., 2013). It is likely that multiple sugar transporters operate for fine-tuning of sugar

425　fluxes for homeostasis and interaction with other proteins for sugar sensing and signaling, including

426　efficient unloading into cell wall spaces, uptake of sucrose or transport via the apoplasm. However,

427　metal exposure concentrations used here might be too low to impact significantly sugar metabolic

428　pathways. Metabolic data thus support that previously observed regulation of genes and proteins

429　involved in sugar metabolism was mostly happening to maintain the level of those metabolites

430　(Regier et al., 2013a; Beauvais-Fluck et al., 2018a; Beauvais-Fluck et al., 2018b).

431

432　**5. CONCLUSION**

433　Metabolomic analysis showed that exposure of *E. nuttallii* to Cd, IHg and MeHg resulted in different

434　metabolomes in each compartment (shoot and cytosol) with some level of coordinated regulation

435　for metabolites between shoots and cytosol. Metabolomic confirmed previous hypothesis of distinct

436　toxicity pathway for IHg and MeHg based on transcriptomics, proteomics and physiology (Larras et

437　al., 2013; Regier et al., 2013a; Beauvais-Fluck et al., 2018a). In contrast to previous proteomics and

438　transcriptomics data, Cd showed a higher impact on individual metabolites, while MeHg impacted

439　more metabolic pathways in shoots, but IHg showed a higher impact in cytosol than MeHg. New

440　omics methods are fundamentally transforming biology approaches, but the fact that many genes

441　and proteins identified by transcriptomics and proteomics have an unknown function results in

442　considerable uncertainty in the analysis of responses. Metabolomics give the opportunity to confirm

443　and reveal effects of toxicants in a complementary way to other omics methods, as it identified early

444　responses that were effective in revealing metal uptake and impact as well as were congruent with

445　expected adverse outcome pathways.

446

449 Rebecca Beauvais-Fluck, Floriane Larras, Beatriz Lobo, Nicole Regier and Debora Tanaami for their

450 help in the management of cultures, sampling of water and the preparation of cytosol extracts.

451

454

REFERENCES

456 Azimi, S., Rocher, V., 2016. Influence of the water quality improvement on fish population in the

457 Seine River (Paris, France) over the 1990-2013 period. Sci Total Environ 542, 955-964.

458 Bailey, N.J., Oven, M., Holmes, E., Nicholson, J.K., Zenk, M.H., 2003. Metabolomic analysis of the

459 consequences of cadmium exposure in *Silene cucubalus* cell cultures via 1H NMR spectroscopy and

460 chemometrics. Phytochemistry 62, 851-858.

461 Banerjee, R., Chen, S., Dare, K., Gilreath, M., Praetorius-Ibba, M., Raina, M., Reynolds, N.M., Rogers,

462 T., Roy, H., Yadavalli, S.S., Ibba, M., 2011. tRNAs: Cellular barcodes for amino acids. FEBS Letters 584,

463 387-395.

464 Beauvais-Fluck, R., Chaumot, A., Gimbert, F., Queau, H., Geffard, O., Slaveykova, V.I., Cosio, C., 2016.

465 Role of cellular compartmentalization in the trophic transfer of mercury species in a freshwater

466 plant-crustacean food chain. Journal of Hazardous Materials 320, 401-407.

467 Beauvais-Fluck, R., Gimbert, F., Mehault, O., Cosio, C., 2017. Trophic fate of inorganic and methyl-

468 mercury in a macrophyte-chironomid food chain. Journal of Hazardous Materials 338, 140-147.

469 Beauvais-Fluck, R., Slaveykova, V.I., Cosio, C., 2018a. Effects of two-hour exposure to environmental

470 and high concentrations of methylmercury on the transcriptome of the macrophyte *Elodea nuttallii*.

471 Aquat Toxicol 194, 103-111.

472 Beauvais-Fluck, R., Slaveykova, V.I., Skyllberg, U., Cosio, C., 2018b. Molecular effects, speciation and

473 competition of inorganic and methyl mercury in the aquatic plant *Elodea nuttallii*. Environmental

474 Science & Technology 52, 8876–8884.

475 Bonanno, G., Lo Giudice, R., 2010. Heavy metal bioaccumulation by the organs of *Phragmites*

476 *australis* (common reed) and their potential use as contamination indicators. Ecological Indicators

477 10, 639-645.

478 Bravo, A.G., Loizeau, J.L., Bouchet, S., Richard, A., Rubin, J.F., Ungureanu, V.G., Amouroux, D.,

479 Dominik, J., 2010. Mercury human exposure through fish consumption in a reservoir contaminated

480 by a chlor-alkali plant: Babeni reservoir (Romania). Environmental Science and Pollution Research

481 17, 1422-1432.

482 Castro, R., Pereira, S., Lima, A., Corticeiro, S., Valega, M., Pereira, E., Duarte, A., Figueira, E., 2009.
483 Accumulation, distribution and cellular partitioning of mercury in several halophytes of a
484 contaminated salt marsh. Chemosphere 76, 1348-1355.

485 Chambers, P.A., Lacoul, P., Murphy, K.J., Thomaz, S.M., 2008. Global diversity of aquatic
486 macrophytes in freshwater. Hydrobiologia 595, 9-26.

487 Cosio, C., Dunand, C., 2010. Transcriptome analysis of various flower and silique development stages
488 indicates a set of class III peroxidase genes potentially involved in pod shattering in *Arabidopsis*
489 *thaliana*. Bmc Genomics 11, 16.

490 Cosio, C., Fluck, R., Regier, N., Slaveykova, V.I., 2014. Effects of macrophytes on the fate of mercury
491 in aquatic systems. Environmental Toxicology and Chemistry 24.

492 Croteau, M.-N., Luoma, S.N., Stewart, A.R., 2005. Trophic transfer of metals along freshwater food
493 webs: Evidence of cadmium biomagnification in nature. Limnology and Oceanography 50, 1511-
494 1519.

495 Fraser, C.M., Chapple, C., 2011. The phenylpropanoid pathway in *Arabidopsis*. The *Arabidopsis* Book
496 / American Society of Plant Biologists 9, e0152.

497 Hayat, S., Hayat, Q., Alyemeni, M.N., Wani, A.S., Pichtel, J., Ahmad, A., 2012. Role of proline under
498 changing environments: A review. Plant Signaling & Behavior 7, 1456-1466.

499 Holcik, M., Sonenberg, N., 2005. Translational control in stress and apoptosis. Nature Reviews
500 Molecular Cell Biology 6, 318.

501 Joshi, V., Joung, J.-G., Fei, Z., Jander, G., 2010. Interdependence of threonine, methionine and
502 isoleucine metabolism in plants: accumulation and transcriptional regulation under abiotic stress.
503 Amino Acids 39, 933-947.

504 Khodayari, S., Moharramipour, S., Larvor, V., Hidalgo, K., Renault, D., 2013. Deciphering the
505 metabolic changes associated with diapause syndrome and cold acclimation in the two-spotted
506 spider mite *Tetranychus urticae*. Plos one 8, e54025-e54025.

507 Kieffer, P., Planchon, S., Oufir, M., Ziebel, J., Dommes, J., Hoffmann, L., Hausman, J.-F., Renaut, J.,
508 2009. Combining proteomics and metabolite analyses To unravel cadmium stress-response in poplar
509 leaves. Journal of Proteome Research 8, 400-417.

510 Larras, F., Regier, N., Planchon, S., Pote, J., Renaut, J., Cosio, C., 2013. Physiological and proteomic
511 changes suggest an important role of cell walls in the high tolerance to metals of *Elodea nuttallii*.
512 Journal of Hazardous Materials 263, 575-583.

513 Lemoine, R., La Camera, S., Atanassova, R., Dedaldechamp, F., Allario, T., Pourtau, N., Bonnemain, J.-
514 L., Laloi, M., Coutos-Thevenot, P., Maurousset, L., Faucher, M., Girousse, C., Lemonnier, P., Parrilla,

515 J., Durand, M., 2013. Source-to-sink transport of sugar and regulation by environmental factors.

516 Frontiers in plant science 4.

517 Liu, B., Yan, H., Wang, C., Li, Q., Guédron, S., Spangenberg, J.E., Feng, X., Dominik, J., 2012. Insights

518 into low fish mercury bioaccumulation in a mercury-contaminated reservoir, Guizhou, China.

519 Environmental Pollution 160, 109-117.

520 Loizeau, J.-L., Edder, P., De Alencastro, L.F., Corvi, C., Ramseier Gentile, S., 2013. La contamination du

521 Léman par les micropolluants - Revue de 40 ans d'études. Archives des Sciences 66, 117-136.

522 Ma, L., Wang, Y., Liu, W., Liu, Z., 2014. Overexpression of an alfalfa GDP-mannose 3, 5-epimerase

523 gene enhances acid, drought and salt tolerance in transgenic *Arabidopsis* by increasing ascorbate

524 accumulation. Biotechnology Letters 36, 2331-2341.

525 Masclaux-Daubresse, C., Reisdorf-Cren, M., Pageau, K., Lelandais, M., Grandjean, O., Kronenberger,

526 J., Valadier, M.-H., Feraud, M., Jouglet, T., Suzuki, A., 2006. Glutamine synthetase-Glutamate

527 synthase pathway and glutamate dehydrogenase play distinct roles in the sink-source nitrogen cycle

528 in Tobacco. Plant Physiology 140, 444-456.

529 Miesak, B.H., Coruzzi, G.M., 2002. Molecular and physiological analysis of *Arabidopsis* mutants

530 defective in cytosolic or chloroplastic aspartate aminotransferase. Plant Physiology 129, 650.

531 Moya, J.L., Ros, R., Picazo, I., 1995. Heavy metal-hormone interactions in rice plants: Effects on

532 growth, net photosynthesis, and carbohydrate distribution. Journal of Plant Growth Regulation 14,

533 61.

534 Niane, B., Guedron, S., Moritz, R., Cosio, C., Ngom, P., Deverajan, N., Pfeifer, H., Pote, J., 2014.

535 Human exposure to mercury in artisanal small-scale gold mining areas of Kedougou region, Senegal,

536 as a function of occupational activity and fish consumption. Environmental Science and Pollution

537 Research, 1-11.

538 Noges, T., Luup, H., Feldmann, T., 2010. Primary production of aquatic macrophytes and their

539 epiphytes in two shallow lakes (Peipsi and Vrtsjarv) in Estonia. Aquatic Ecology 44, 83-92.

540 Obata, T., Fernie, A.R., 2012. The use of metabolomics to dissect plant responses to abiotic stresses.

541 Cellular and Molecular Life Sciences 69, 3225-3243.

542 Patrick, J., Botha, F., Birch, R., 2013. Metabolic engineering of sugars and simple sugar derivatives in

543 plants. Plant Biotechnology Journal 11, 142-156.

544 Pavlikova, D., Pavlik, M., Staszkova, L., Motyka, V., Szakova, J., Tlustos, P., Balik, J., 2008. Glutamate

545 kinase as a potential biomarker of heavy metal stress in plants. Ecotoxicol Environ Saf 70, 223-230.

546 Piotrowska, A., Bajguz, A., Godlewska-Zylkiewicz, B., Zambrzycka, E., 2010. Changes in growth,

547 biochemical components, and antioxidant activity in aquatic plant *Wolffia arrhiza* (Lemnaceae)

548 exposed to cadmium and lead. Archives of Environmental Contamination and Toxicology 58, 594-
549 604.

550 Raina, M., Ibba, M., 2014. tRNAs as regulators of biological processes. Front Genet 5.

551 Regier, N., Baerlocher, L., Munsterkotter, M., Farinelli, L., Cosio, C., 2013a. Analysis of the *Elodea*
552 *nuttallii* transcriptome in response to mercury and cadmium pollution: development of sensitive
553 tools for rapid ecotoxicological testing. Environmental Science & Technology 47, 8825-8834.

554 Regier, N., Beauvais-Flück, R., Slaveykova, V.I., Cosio, C., 2016. *Elodea nuttallii* exposure to mercury
555 exposure under enhanced ultraviolet radiation: Effects on bioaccumulation, transcriptome, pigment
556 content and oxidative stress. Aquatic Toxicology 180, 218-226.

557 Regier, N., Larras, F., Bravo, A.G., Ungureanu, V.G., Amouroux, D., Cosio, C., 2013b. Mercury
558 bioaccumulation in the aquatic plant *Elodea nuttallii* in the field and in microcosm: accumulation in
559 shoots from the water might involve copper transporters. Chemosphere 90, 595-602.

560 Renault, D., Puzin, C., Foucreau, N., Bouchereau, A., Petillon, J., 2016. Chronic exposure to soil
561 salinity in terrestrial species: Does plasticity and underlying physiology differ among specialized
562 ground-dwelling spiders? Journal of Insect Physiology 90, 49-58.

563 Renault, H., Roussel, V., El Amrani, A., Arzel, M., Renault, D., Bouchereau, A., Deleu, C., 2010. The
564 *Arabidopsis* pop2-1mutant reveals the involvement of GABA transaminase in salt stress tolerance.
565 BMC Plant Biology 10, 20.

566 Rizhsky, L., Liang, H., Shuman, J., Shulaev, V., Davletova, S., Mittler, R., 2004. When defense
567 pathways collide. The response of *Arabidopsis* to a combination of drought and heat stress. Plant
568 Physiology 134, 1683-1696.

569 Rosa, M., Prado, C., Podazza, G., Interdonato, R., Gonzalez, J.A., Hilal, M., Prado, F.E., 2009a. Soluble
570 sugars--metabolism, sensing and abiotic stress: a complex network in the life of plants. Plant
571 Signaling & Behavior 4, 388-393.

572 Rosa, M., Prado, C., Podazza, G., Interdonato, R., Gonzalez, J.A., Hilal, M., Prado, F.E., 2009b. Soluble
573 sugars--metabolism, sensing and abiotic stress: a complex network in the life of plants. Plant
574 Signaling & Behavior 4, 388-393.

575 Samecka-Cymerman, A., Kempers, A.J., 2003. Biomonitoring of water pollution with *Elodea*
576 *canadensis*. A case study of three small Polish rivers with different levels of pollution. Water Air and
577 Soil Pollution 145, 139-153.

578 Stoichev, T., Martin-Doimeadios, R.C.R., Tessier, E., Amouroux, D., Donard, O.F.X., 2004.
579 Improvement of analytical performances for mercury speciation by on-line derivatization,
580 cryofocussing and atomic fluorescence spectrometry. Talanta 62, 433-438.

581 Tohge, T., Scossa, F., Fernie, A.R., 2015. Integrative approaches to enhance understanding of plant
582 metabolic pathway structure and regulation. Plant Physiology 169, 1499.

583 Topfer, N., Scossa, F., Fernie, A., Nikoloski, Z., 2014. Variability of metabolite levels is linked to
584 differential metabolic pathways in *Arabidopsis*'s responses to abiotic Stresses. PLOS Computational
585 Biology 10, e1003656.

586 Tzin, V., Galili, G., 2010. The biosynthetic pathways for shikimate and aromatic amino acids in
587 *Arabidopsis thaliana*. The arabidopsis book 8, e0132-e0132.

588 Valega, M., Lima, A.I.G., Figueira, E., Pereira, E., Pardal, M.A., Duarte, A.C., 2009. Mercury
589 intracellular partitioning and chelation in a salt marsh plant, Halimione portulacoides (L.) Aellen:
590 Strategies underlying tolerance in environmental exposure. Chemosphere 74, 530-536.

591 Venkatesh, J., Park, S.W., 2014. Role of L-ascorbate in alleviating abiotic stresses in crop plants.
592 Botanical Studies 55, 38.

593 Vital, C.E., Giordano, A., de Almeida Soares, E., Rhys Williams, T.C., Mesquita, R.O., Vidigal, P.M.P.,
594 de Santana Lopes, A., Pacheco, T.G., Rogalski, M., de Oliveira Ramos, H.J., Loureiro, M.E., 2017. An
595 integrative overview of the molecular and physiological responses of sugarcane under drought
596 conditions. Plant Molecular Biology 94, 577-594.

597 Wetzel, R.G., 2001. Limnology – lake and river ecosystems (3rd edition). Academic Press, San Diego.

598 Xu, J., Sun, J., Du, L., Liu, X., 2012. Comparative transcriptome analysis of cadmium responses in
599 *Solanum nigrum* and *Solanum torvum*. New Phytologist 196, 110-124.

600 Yancey, P.H., 2005. Organic osmolytes as compatible, metabolic and counteracting cytoprotectants
601 in high osmolarity and other stresses. Journal of Experimental Biology 208, 2819.

602 Zemanova, V., Pavlik, M., Pavlikova, D., 2017. Cadmium toxicity induced contrasting patterns of
603 concentrations of free sarcosine, specific amino acids and selected microelements in two *Noccaea*
604 species. Plos one 12, e0177963.

605 Zhang, Z., Mao, C., Shi, Z., Kou, X., 2017. The amino acid metabolic and carbohydrate metabolic
606 pathway play important roles during salt-stress response in Tomato. Frontiers in plant science 8,
607 1231-1231.

608

609

610

611 **Table 1**. Lignin content, chloropyll content, performance index of PSII [PI(abs)], class III peroxidase

612 [POD] and superoxide dismutase [SOD] activities and bioaccumulation in shoots of *Elodea nuttallii*

613 exposed to 280 μg·L^{-1} Cd, 70 ng·L^{-1} IHg, or 30 ng·L^{-1} MeHg or not (control). For each treatment, three

614 replicates were analyzed. Data are presented as mean ± standard deviation (SD; n= 3). Bold font = p-

615 value <0.05 relative to control plants.

	Shoots					Bioaccumulation		
	Lignin content	Chlorophyll	PI (abs)	POD	SOD	IHg	MeHg	Cd
	(μg·mg^{-1} fresh mass)			(nkat·mg^{-1} protein)	(units·μg^{-1} protein)	(μg·g^{-1} dry mass)		
Control	7.2 ± 1.3	0.90 ± 0.27	0.79 ± 0.02	18.4 ± 1.63	0.93 ± 0.08	0.03 ± 0.03	0.01 ± 0.01	0.82 ± 0.12
Cd	6.4 ± 1.4	0.78 ± 0.30	0.80 ± 0.01	28.5 ± 5.6	1.04 ± 0.06	NA	NA	**921 ± 28**
IHg	5.6 ± 1.3	0.75 ± 0.16	0.79 ± 0.02	17.0 ± 1.4	1.08 ± 0.05	**0.97 ± 0.11**	0.01 ±0.01	NA
MeHg	5.6 ± 2.2	0.88 ± 0.23	0.80 ± 0.01	18.3 ± 6.03	1.01 ± 0.08	**0.14 ± 0.03**	0.67 ± 0.11	NA

616 NA (not analyzed).

617

618

619 **Table 2.** Concentration (nmoles·mg^{-1} dry mass) of amino acids, organic acids, polyols and sugars

620 (n=3; mean ± SD) whose levels significantly varied in shoots of *E. nuttallii* exposed for 24h to Cd, IHg

621 and MeHg (bold font = p-value <0.05), relative to control plants.

	Control	Cd	IHg	MeHg
Ammonium	4.21 ±1.03	6.12 ± 2.35	3.90 ± 0.89	**7.72 ± 2.06**
Aspartic Acid	15.22 ± 2.79	**0.72 ± 0.84**	13.41 ± 2.44	**21.77 ± 1.77**
BABA	0.02 ± 0.01	**0.09 ± 0.06**	0.07 ± 0.05	**0.08 ± 0.06**
Glutamine	9.03 ± 2.06	6.73 ± 1.61	8.87 ± 2.13	**14.61 ± 4.43**
Glycine	1.20 ± 0.20	1.00 ± 1.43	0.97 ± 0.23	**1.96 ± 0.30**
Histidine	0.38 ± 0.12	**1.36 ± 0.45**	0.30 ± 0.07	0.47 ± 0.19
Hydroxyproline	0.00 ± 0.00	0.04 ± 0.04	0.01 ± 0.01	**0.02 ± 0.01**
Isoleucine	0.24 ± 0.17	**3.73 ± 1.14**	0.15 ± 0.12	0.40 ± 0.24
Leucine	0.17 ± 0.08	**2.74 ± 0.70**	0.12 ± 0.05	**0.28 ± 0.08**
Lysine	0.25 ± 0.21	**1.22 ± 0.42**	0.18 ± 0.18	0.41 ± 0.34
Methionine	0.03 ± 0.01	0.04 ± 0.01	0.03 ± 0.01	**0.06 ± 0.01**
Methylcysteine	0.10 ± 0.05	**0.03 ± 0.03**	0.07 ± 0.03	0.11 ± 0.04
Phenylalanine	0.38 ± 0.08	**2.15 ± 0.78**	0.34 ± 0.03	**0.66 ± 0.15**
Proline	0.39 ± 0.15	**1.93 ± 0.46**	0.30 ± 0.13	**0.64 ± 0.23**
Serine	4.49 ± 1.05	4.64 ± 0.56	4.29 ± 1.03	**7.21 ± 1.02**
Threonine	1.91 ± 0.37	**5.68 ± 1.72**	1.73 ± 0.35	**3.08 ± 0.47**
Tryptophan	0.10 ± 0.02	**1.60 ± 0.33**	0.12 ± 0.05	**0.21 ± 0.03**
Tyrosine	0.14 ± 0.04	**1.54 ± 0.38**	0.12 ± 0.03	**0.24 ± 0.03**
Valine	0.52 ± 0.28	**5.24 ± 1.44**	0.37 ± 0.24	0.82 ± 0.41
Adonitol	0.45 ± 0.09	**1.07 ± 0.31**	0.46 ± 0.07	0.44 ± 0.08
Arabinose	0.65 ± 0.20	**0.95 ± 0.19**	0.59 ± 0.09	0.47 ± 0.07
Arabitol	0.28 ± 0.04	0.23 ± 0.04	0.18 ± 0.04	**0.15 ± 0.03**
Pipecolic Acid	0.65 ± 0.20	**0.95 ± 0.19**	0.59 ± 0.09	0.47 ± 0.08
Ribose	2.81 ± 1.02	**5.43 ± 1.39**	3.02 ± 0.74	3.46 ± 1.19

622

623

624

625 **Table 3**. Concentration (nmoles·mg^{-1} dry mass) of amino acids, organic acids, polyols and sugars

626 (n=3; mean ± SD) whose amounts significantly varied (relative to control) in the cytosol of *E. nuttallii*

627 exposed for 24h to Cd, IHg and MeHg (bold font = p-value <0.05).

|	Control	Cd	IHg	MeHg
Alpha-alanine	0.48 ± 0.01	**0.31 ± 0.05**	0.50 ± 0.17	0.33 ± 0.18
Ammonium	0.52 ± 0.13	**0.89 ± 0.11**	**0.81 ±0.07**	0.62 ± 0.32
Arginine	0.16 ± 0.02	0.05 ± 0.06	**0.02 ± 0.01**	**0.04 ± 0.04**
Aspartic Acid	1.22 ± 0.12	**0.60 ± 0.11**	1.23 ± 0.41	0.77 ± 0.44
Glycine	0.18 ± 0.03	**0.40 ± 0.03**	0.12 ± 0.03	0.19 ± 0.15
Histidine	0.14 ± 0.01	0.58 ± 0.99	0.07 ± 0.01	**0.0 ± 0.0**
Hydroxyproline	3.68 ± 0.25	**5.89 ± 0.84**	4.42 ± 0.83	3.84 ± 2.01
Galactose	0.99 ± 0.01	**0.39 ± 0.03**	0.63 ± 0.21	**0.35 ± 0.17**
Mannose	0.08 ± 0.01	**0.02 ± 0.01**	**0.04 ± 0.02**	**0.03 ± 0.01**
Phosphoric acid	6.89 ± 1.26	**15.20 ± 3.09**	7.31 ± 0.82	7.26 ± 3.35

628

629

630

631

632

633
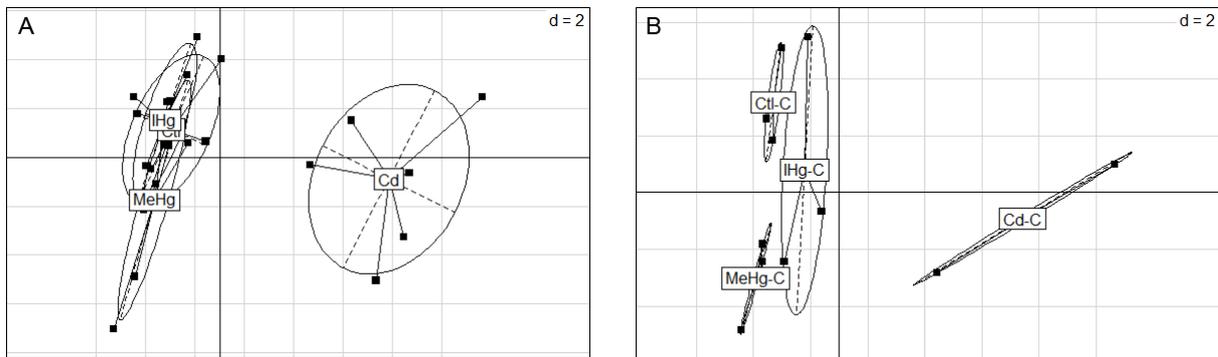
Figure 1. Principal component analysis of amino acids, organic acids, sugars and polyols measured in shoots (A) and cytosol (B) of *E. nuttallii* exposed 24h to 281 µg·L^{-1} Cd, 70 ng·L^{-1} IHg and 30 ng·L^{-1} MeHg, and their control (ctl) (n=6 and 3 ± SD, respectively). PCA were calculated and plotted with the package ade4 (http://pbil.univ-lyon1.fr/ade4) in the R software (http://www.r-project.org).

634

- Cd, IHg and MeHg effects were compared in shoots and cytosol by metabolomics

- In shoots, Cd showed higher regulation, but MeHg regulated more pathways

- In cytosol, Cd had the higher impact, IHg had low effect and MeHg had very low effect

- MeHg impacts N homeostasis, and Cd results in an osmotic stress-like pattern

- Metabolomics support different molecular toxicity pathways for the three metals

Authors declare no conflict of interest